

# Centralized Fiber-Fault Surveillance System for PONs using Low Cost Coding

Habib Fathallah<sup>(\*)</sup>

Dept. of Electrical Engineering, College of Engineering,  
King Saud University, P.O. Box 800,  
Riyadh 11421, Saudi Arabia  
hfathallah@ksu.edu.sa

Mohammad M. Rad, and Leslie A. Rusch

Centre d'Optique Photonique et Laser,  
Université Laval,  
Québec (Qc), G1K 7P4, Canada

**Abstract**—We propose a novel dual Bragg gratings cavity based coding for centralized fiber-fault surveillance of passive optical networks (PONs). This reduces the cost of manufacturing, installation, inventory, and operation, while maintaining good performance and capacity.

*PON, Network Management, FTTX, FTTH, Fiber-Fault Monitoring.*

## I. INTRODUCTION

Surveillance of standard fiber-to-the-home-passive optical networks (FTTH-PON) is a serious open question. Some service providers report that more than 80% of installed PON failures occurs within the first/last mile, i.e., within the distribution/drop segments of the network. When a fault occurs, technicians must be dispatched to identify, locate and fix the failure. The time, labor and truck-roll for fault identification dramatically increase the operational expenditure (OPEX) and erode profit margin. Furthermore, long repair time causes customer dissatisfaction and complaints. Therefore, a centralized surveillance, i.e., from the central office (CO) is highly desired because it provides instantaneous, full in-service information and control for service providers [1-5].

It is well known that optical-time-domain reflectometry (OTDR) is inefficient for point-to-multipoint (PMP) networks like PONs since it is not capable to identify a specific broken branch in the PON tree architecture [1-3]. Few solutions exist for the monitoring of a PON. While imposing significant technical challenges, most techniques are impractical due to their limited capacity (few customers) [2-5]. In [6-7], we introduced, for the first time, a modified optical code division multiplexing (OCDM) scheme for centralized monitoring of PONs that is architecture agnostic. In this system, no active component is placed in the field and no intelligent module is embedded inside the customer's optical network terminal (ONT). In all our previous studies we only considered standard OCDMA coding schemes [8].

and lower cost optical coding devices. Recall that the PON market is very cost-sensitive, particularly for network elements not shared between customers, i.e., ONTs, DDF, and passive coding devices for monitoring of each DDF. Our results show that our new proposal supports the monitoring of a 64 customer PON with SNR>10 dB.

## II. PRINCIPLE OF OPTICAL CODING SURVEILLANCE SYSTEM

As illustrated in Fig. 1a, a U band short pulse with peak power  $P_s$  and duration  $T_s$  is transmitted through the feeder, split into  $N$  sub-pulses at the remote node (RN), each of which is encoded and reflected back to the CO by a dual function device: encoder and mirror, we refer to as coding mirror ( $CM_i$ ,  $i = 1, \dots, N$ ). Each DDF drop is terminated by a CM with a unique code, and is located physically close to the ONT. Information on individual DDFs is discernable at the CO due to the near orthogonality of the codes. The CO monitoring equipment decodes the received signal for the target line; a healthy target DDF contributes an auto-correlation peak, while

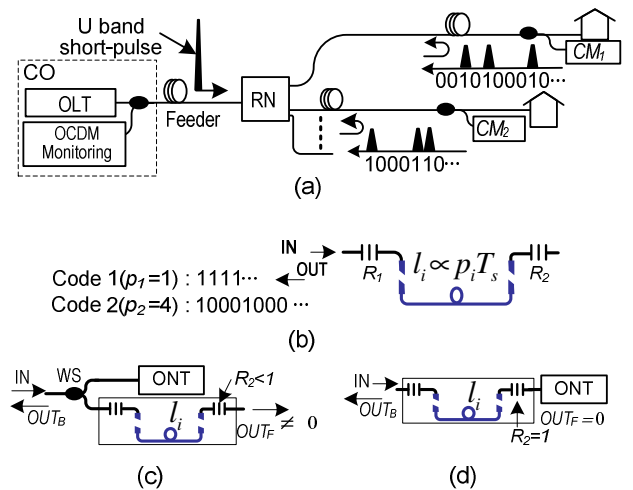


**Fig. 1: (a) Optical coding monitoring system, (b) proposed CM structure, and two CM solutions (c) and (d).**

(\*) The author acknowledges the contribution of the Research center of the (College of Engineering, KSU).

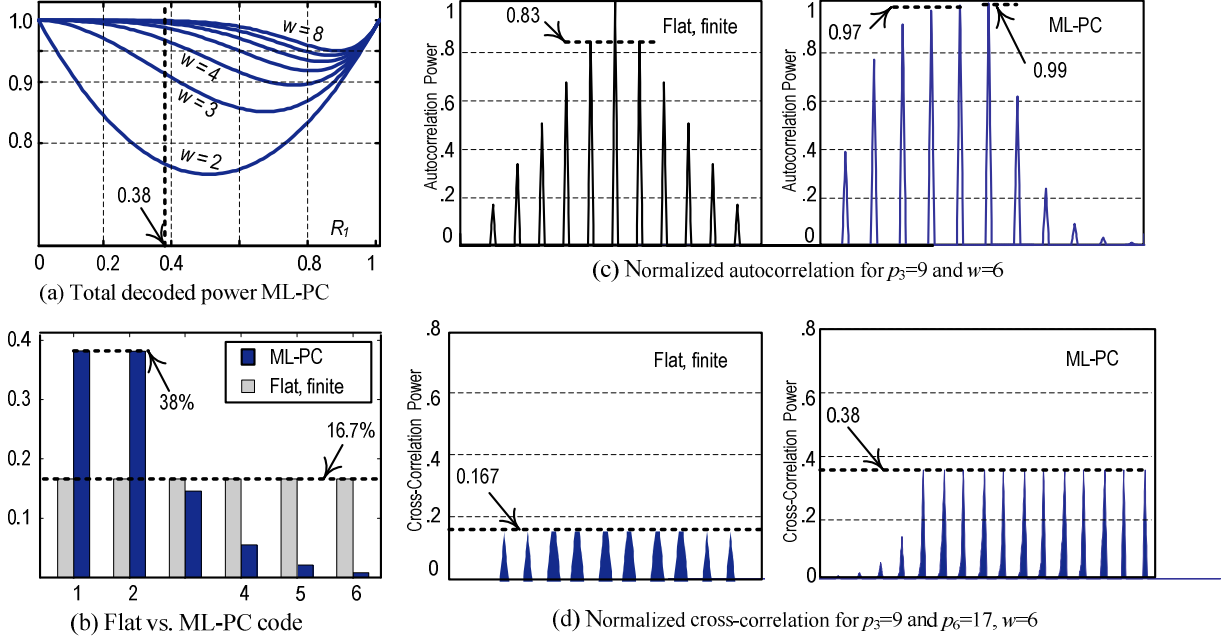


**Fig. 2. Example of a flat, finite code and an ML-PC code.**

non-targeted DDFs contribute cross-correlation spikes.

In [6–8], we considered the CO monitoring equipment with a programmable decoder that correlates the received signal cyclically for each subscriber line. The correlated (or decoded) signal is then photo-detected, and the autocorrelation peak is identified by an electric threshold that rejects cross-correlation spikes and noise.

In this paper, however, we propose the decoding functions be implemented in electronics after the photodetector. Our PON monitoring system exploits short pulses (sub nanosecond to a few nanoseconds). The gigahertz speed electronics required are economically feasible today, especially for the CO equipment whose cost can be amortized over the client base. In addition to reducing the cost of the monitoring system, electronic decoding eliminates the power insertion and decoding loss, hence alleviating the loss/power budget of the system. Furthermore, electronic decoding reduces substantially the so-called beat noise that limits performance of OCDM systems.

### III. NOVEL CODING MIRRORS BASED ON OPTICAL CAVITY

All previously proposed CMs are composed of high loss passive splitters or a series of Bragg gratings as in standard OCDM systems [6]. These schemes require a wavelength selector (WS) multiplexing/demultiplexing the U band from data bands at the CO and DDF terminations. Moreover, they involve high manufacturing, splicing, and packaging complexity, increasing the cost of the installation, repair and inventory.

In this paper, we propose a new simple coding structure that exploits only two Bragg gratings written for the same wavelength and forming an optical cavity (see Fig. 1b). A

single incident pulse generates an infinite sequence of equally spaced multilevel pulses in reflection. We further suppose that each subscriber has a pair of Bragg gratings with the same reflectivities  $R_1$  and  $R_2$ , and the same center wavelength. Only a unique physical separation  $l_i$  of the grating distinguishes one subscriber from the next, i.e., each subscriber has a unique cavity length. We refer to the code generated by this cavity as a multilevel periodic code (ML-PC).

An ML-PC is thus determined by the length of the silent intervals separating the multilevel pulses, i.e., its period. The period of the  $i_{th}$  code is unique and related to the cavity length  $l_i$  by

$$p_i \triangleq 2 \frac{nl_i}{cT_s}, \quad i = 1, 2, \dots, N \quad (1)$$

given in units of pulse duration, where  $n$  is the effective group index and  $c$  is the speed of light in the fiber core. The fiber length inserted between gratings fixes cavity length and differentiates the codes. In Fig. 1b, we show a logical description of periodic codes for  $p_1 = 1$  and  $p_2 = 4$ . When  $T_s = 1$  ns,  $l_1$  and  $l_2$  equal 10 cm and 40 cm respectively.

Fig. 1c and 1d illustrate two solutions for our cavity based CM. The first allows  $R_2$  to be inferior to one, so the incident pulse power can be split between backward (OUTB) and forward (OUTF) paths. This scheme allows greater flexibility in using  $R_1$  and  $R_2$  to fix code pulse levels, however insertion loss is non-negligible and a WS is required [6].

The second solution fixes  $R_2 = 1$ , constraining all power to be reflected back to the CO (i.e.,  $OUT_F = 0$ ). This reduces CM cost as no WS is needed, and improves power budget. In the following, we focus on the latter scheme. When  $R_2$  is fixed to one, only  $R_1$  dictates these levels of the code pulses when

neglecting cavity length induced loss. Let  $\rho_j$  be the height (or level) of the  $j^{\text{th}}$  pulse generated by the cavity. We find  $\rho_j$  from

$$\rho_j = \begin{cases} R_1 & j=1 \\ (1-R_1)^2 R_2 & j \geq 2 \end{cases} \quad (2)$$

As an optimization criterion, we seek to concentrate reflected power in a few pulses. This avoids long codes with greater interference between codes. Fig. 2a illustrates the total power contained in the first  $w$  pulses of the sequence as a function of  $R_1$ . The ML-PC code (dark bars) illustrated in Fig. 2b corresponds to  $w = 6$  and  $R_1 = 0.38$ , ensuring 99% of the incident pulse power is reflected in the first six pulses.

The simple structure of our PCs enables us to produce any desired number of codes no matter constraints on code weight and correlation. We developed a simple algorithm, for determining the codes:

- (i) knowing the desired code weight  $w$ , we obtain the first code corresponding to a period  $p_1 = 1$ ;
- (ii) the  $i^{\text{th}}$  code has period  $p_i = p_{i-1} + 1$  if its maximum cross-correlation with all the  $k^{\text{th}}$  codes ( $k=1, \dots, i-1$ ) is one, otherwise we increment  $p_i$  until meeting this cross-correlation constraint.

#### IV. ML-PC CODE PROPERTIES

ML-PC codes have infinite length, but pulse heights die out exponentially. We assume the receiver has perfect knowledge of the observation window, *i.e.*, the timing of the autocorrelation peak, or equivalently, the exact location of the desired customer in the network. We consider ML-PC codes with power concentrated into a small number of  $w$  pulses. Fig. 2b shows a truncated version of a ML-PC (dark bars); the first  $w = 6$  pulses contain 99% of the total code power. For simplicity we always normalize the total code power to one. We also assume the decoder correlates the received signal with the truncated version of the code;  $w = 6$  being the weight of the decoder. In Fig. 2b, for comparison with the ML-PC code (dark bars) we also consider a flat, finite, weight 6 code (gray bars). Note the flat, finite code is not achievable with our cavity encoder.

In Fig. 2c, we give the autocorrelation function for code  $p_3 = 9$  for both ML-PC and flat infinite codes. We observe a main lobe equal to one for flat finite codes corresponding to the sum of six equal pulses, and 0.99 for ML-PC equal to the sum of its six unequal pulses. We see high out-of-phase side-lobes with a maximum corresponding to the superposition of  $w-1$  pulses (similar to standard prime codes). For flat finite PC this is equal to  $(w-1)/w=0.83$  however for ML-PC this is equal to 0.97, the sum of its highest five pulses. High side lobes are undesirable for standard OCDMA as it increases the inter-symbol interference.

In our application this property is acceptable as we do not transmit streams of data. Proper choice of weight and period can limit the maximum cross-correlation to one pulse as discussed previously. One pulse cross-correlation is desirable for both monitoring and standard OCDMA. The cross-correlation examples in Fig. 2d consider codes with

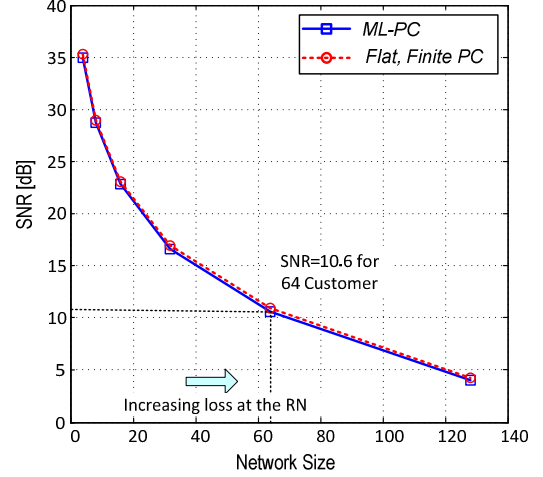


Fig. 3: SNR of binary vs. multilevel periodic coding.

periods  $p_3 = 9$  and  $p_6 = 17$ . We obtain unitary cross-correlation, *i.e.*,  $1/6=0.167$  for flat finite codes and 0.38 for ML-PC.

#### V. SNR VS CAPACITY EVALUATION

In order to assess the performance of this monitoring technique with the proposed multilevel codes we consider the following expression for the signal-to-noise ratio (SNR),

$$SNR \triangleq \frac{\mu_{SIG}^2}{\sigma_N^2} \triangleq \frac{\mu_{SIG}^2}{\sigma_{TH}^2 + \sigma_D^2 + \sigma_{SH}^2 + \sigma_{BN}^2} \quad (3)$$

where  $\mu_{SIG}$  and  $\sigma_N^2$  are, respectively, the useful signal and total noise power in the autocorrelation main lobe. Index TH is used for thermal noise (spectral density 0.1 pA.Hz-0.5), D for dark current (average current 160 nA), SH for shot noise and BN for beat noise (this include the interference noise). A coherent laser source at  $\lambda = 1650\text{nm}$  corresponding to 0.3 dB/km fiber loss is assumed. We also considered  $T_s = 1$  ns and  $P_s = 4$  dBm. To compensate the system loss, we use an avalanche photodiode (APD) with gain=100 and excess noise factor=7.9. We considered an aggregate excess loss of 5dB for splicing, connectors, etc. The clients are considered to be uniformly distributed over 1 km<sup>2</sup> coverage area after a 20 km feeder [7].

In Fig. 3, we illustrate the SNR as a function of the number of customers. For a 64 customer PON, the proposed ML-PCs achieve 10.6 dB SNR; this represents less than 1 dB penalty compared to the binary, flat, finite code. Negligible difference exists between binary and multilevel PCs. This result is intuitively true because for the multilevel PC the autocorrelation main lobe includes 0.99 of the desired power compared to the binary codes.

#### VI. CONCLUSION

We proposed and analyzed a new optical coding device that trades suboptimum performance in high capacity PONs for reducing the capital (CAPEX) and operating (OPEX) expenses of PON monitoring system. An SNR of 10 dB is

achieved for a 64 customer PON with households randomly distributed over the 1 km<sup>2</sup> coverage area.

#### REFERENCES

- [1] A. Girard, *FTTx PON Technology and Testing*, EXFO Electro-Optical Engineering Inc., Canada 2005, ISBN 1-55342-006-3.
- [2] D. Iida, *et al.*, "Design of identification fibers with individually assigned...", *IEEE J. Light. Tech.*, vol. 25, no. 5, pp. 1290-1297, May 2007.
- [3] S. Hann, "Monitoring technique for a hybrid PS/WDM-PON ...," *Meas. Science Technology*, 17, pp. 1070-1074, 2006.
- [4] C. Yeh, *et al.*, "Optical fiber-fault surveillance for ...," *Optics Express*, vol. 13, no. 14, pp. 5494-5498, July 2005.
- [5] S. B. Park, *et al.*, "Optical fault monitoring method using ...," *IEE Electronic Letter*, vol. 42, no. 4, Feb. 2006.
- [6] H. Fathallah, *et al.*, "Code-division multiplexing for in-service ...," *J. Optical Networking*, vol. 6, no. 7, July 2007.
- [7] M. Rad, *et al.*, "Effect of PON geographical distribution on ...," *ECOC Sep. 2007*, Germany.
- [8] M. Rad, *et al.*, "Beat Noise Mitigation via Hybrid 1D/2D-OCDM...", OFC, OMR7, San Diego, USA, Feb. 2008.
- [9] H. Fathallah, *et al.*, "PON Monitoring: Periodic Encoders with low...", *Photonic Technology Letter*, 15 December 2008.